Reactions $^{12}C(\pi^{\pm},\pi^{\pm}d)^{10}B$ and $^{12}C(\pi^{\pm},\pi^{\pm}t)^{9}B$

R. J. Ellis,* H. J. Ziock,† K. O. H. Ziock, and Y. Tzeng‡
Physics Department, University of Virginia, Charlottesville, Virginia 22901

J. Arvieux§
Institut des Sciences Nucléaires, Université de Grenoble, BP 257, F-38044 Grenoble-Cedex, France

R. Corfu and J. Piffaretti
Institute de Physique, Université de Neuchatel, CH-2000 Neuchatel, Switzerland

L. C. Liu and E. R. Siciliano||
Los Alamos National Laboratory, Los Alamos, New Mexico 87545
(Received 21 June 1982)

We have measured the angular and momentum distributions of the scattered pions from the reaction $^{12}C(\pi^{+},\pi^{+}d)^{10}B$ in a coincidence experiment. We compare our results with two theoretical models based on the impulse approximation. We also present some data on the reactions $^{12}C(\pi^{\pm},\pi^{\pm}t)^{9}B$.

[NUCLEAR REACTIONS $^{12}C(\pi^{\pm},\pi^{\pm}d)^{10}B$, $^{12}C(\pi^{\pm},\pi^{\pm}t)^{9}B$, $E_{\pi}=130$, 150 MeV; measured $\sigma(p)$, $\sigma(\theta)$, compared with PWIA.]

I. INTRODUCTION

While studying the reactions $^{12}C(\pi^{\pm},\pi^{\pm}p)^{11}B$ we also obtained some data on the reactions $^{12}C(\pi^{\pm},\pi^{\pm}d)^{10}B$ and $^{12}C(\pi^{\pm},\pi^{\pm}t)^{9}B$. A preliminary account of the $(\pi^{\pm},\pi^{\pm}d,t)$ measurements was given in an earlier paper.[1] Here we present angular and momentum distributions and compare them with two theoretical models. The first, or "one step model," assumes a one step process in which a proton and neutron, whose wave functions overlap, are ejected together [see Fig. 1(a)]. The second, or "two step model," assumes that a single nucleon is knocked out in a quasifree scattering process and that this nucleon subsequently picks up one of the other nucleons [see Fig. 1(b)] to form a deuteron.

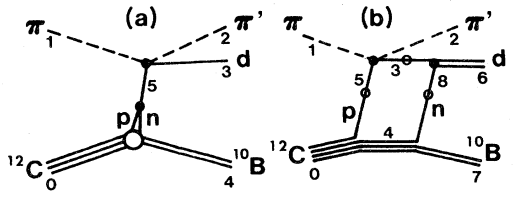

FIG. 1. Diagrams of the reaction $^{12}C(\pi,\pi d)^{10}B$: (a) the one-step model; (b) the two-step model. There is an equivalent diagram to (b) in which the roles of the intermediate proton and neutron are interchanged. The internal particles marked with a circle are assumed to be on their mass shells.

II. DESCRIPTION OF THE EXPERIMENT

The experiment was carried out at the $\pi M1$ pion channel of the Schweizerisches Institut für Nuklearforschung (SIN).[2] The scattered pions were

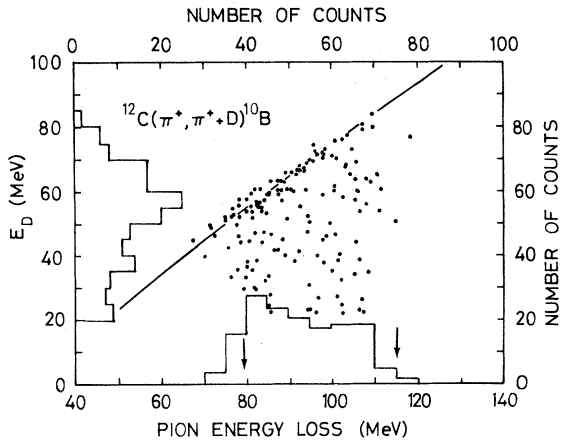

FIG. 2. Scatter plot of the energy of the ejected deuteron versus the pion energy loss in the reaction $^{12}C(\pi^{+},\pi^{+}d)^{10}B$.

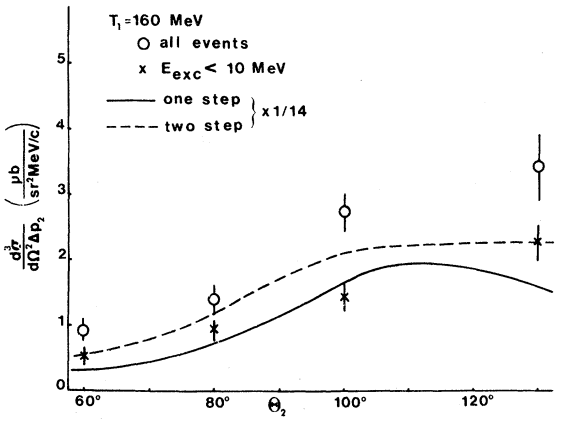

FIG. 3. Measured cross section versus θ_2 for the reaction $^{12}C(\pi^{\pm},\pi^{\pm},d)^{10}B$ for $E_x<10$ MeV for $T_1=160$ MeV. The solid curve represents the one-step model and the dashed curve the two-step model. The use of the symbol Δp_2 indicates integration over a rather large momentum bite ($\Delta p=61$ MeV/c), multiplied by an empirical normalization factor as indicated.

momentum analyzed with SUSI (SIN Universal Spectrometer Installation).[3] In coincidence with "SUSI" we used a four element Si-Ge spectrometer to identify the deuterons and tritons, and to measure their energy. Except where noted otherwise, the SUSI spectrometer was tuned to a central momentum of 169.5 MeV/c (80 MeV). The Si-Ge spectometer was held at an angle of 30° with respect to the incident beam. The angle of SUSI was varied as indicated (all angles are given in the laboratory frame). For a more detailed description of the experimental setup as well as for a discussion of the

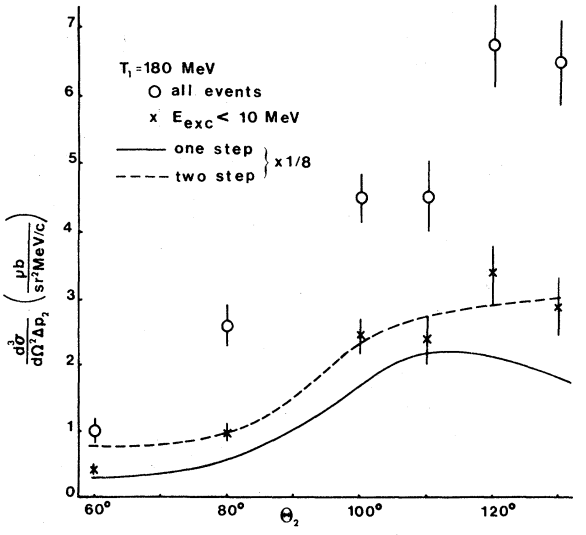

FIG. 4. Same as Fig. 3 except that $T_1=180$ MeV.

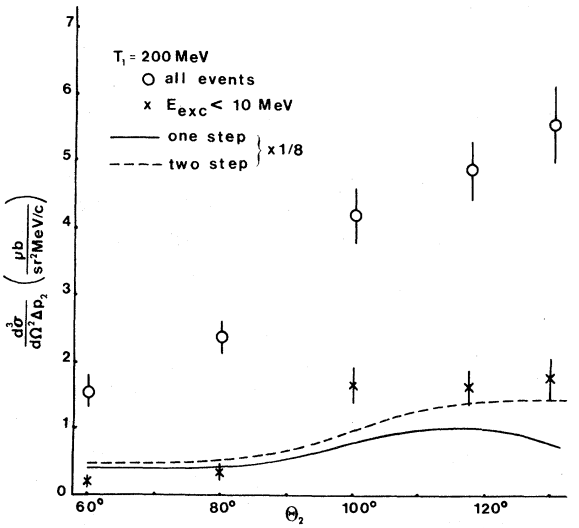

FIG. 5. Same as Fig. 3 except that $T_1=200$ MeV.

kinematics we refer to Refs. 1, 4, and 5.

The results of a typical run are shown in Fig. 2. The data are clipped at high and low pion energies by the momentum bite of SUSI. The arrows indicate where the SUSI acceptance fell to 50% of its central value. A low energy cutoff caused by range effects in the Si-Ge spectrometer can be seen in the

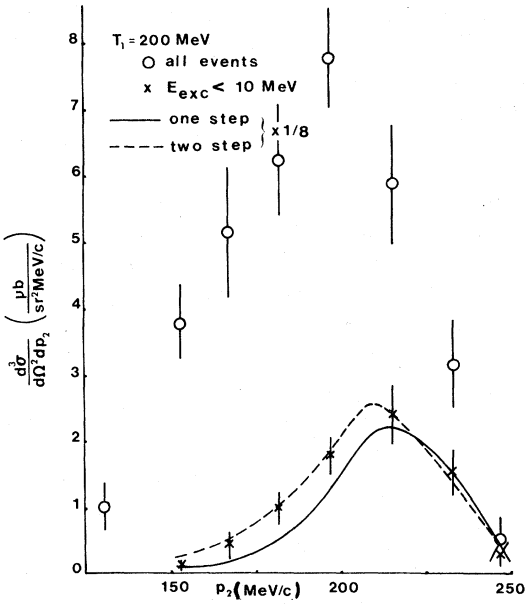

FIG. 6. Measured cross section versus p_2 for the reaction $^{12}C(\pi^{+},\pi^{+}d)^{10}B$ for $T_1=200$ MeV and $\theta_2=117.5°$ for all the data (circles) and for $E_x<10$ MeV (crosses). The solid curve represents the one-step model and the dashed curve represents the two-step model, multiplied by an empirical normalization factor as indicated.

deuteron energy spectrum.

The curve is the locus for all those events that left the residual nucleus in its ground state. The clustering of the events in the vicinity of this curve indicates that roughly 50% of the events lead to the ground state or to one of the lower excited states of the residual ^{10}B nucleus. As in Ref. 1 we have divided our data according to the excitation energy E_{ex} of the residual ^{10}B nucleus. Events with $E_{ex} \leq 10$ MeV leave the residual nucleus in the ground state or one of the lower excited states.

For events with $E_{ex} > 10$ MeV the residual nucleus is excited into the continuum. The latter events are either due to the knockout of a nucleon from one of the deeper shells or to more violent final state interactions. They should not be well described by our models, which are based on an impulse approximation. The comparison between theory and experiment in Figs. 3–6 should thus be made with those experimental points ($\times$) that represent only the events with $E_{ex} \leq 10$ MeV.

Figures 3–5 show the angular distributions of the scattered pions from the reaction ^{12}C$(\pi^+,\pi^+d)^{10}$B for incident pion energies of 160, 180, and 200 MeV, respectively. The solid and the dashed curves represent our calculations in the one-step and two-step models as defined in Sec. III. The cross section $d^3\sigma/d\Omega_\pi d\Omega_d dp_\pi$ is, in actuality, more nearly a double differential cross section since we have averaged over a momentum bite of 61 MeV/c.

As in all impulse approximation calculations that do not take into account distortion effects, the theoretical cross sections are much too large. The neglected effects, mainly the loss of pion flux to other reaction channels, can be shown to have little dependence on scattering angle or pion momentum.[6,7] This discrepancy, for which we have accounted by introducing an empirical normalization factor, should, therefore, be of little importance and in the comparison between theory and experiment one should concentrate on similarities of shape, rather than on absolute magnitudes.

In Fig. 6 we have plotted the cross section as a function of the momentum of the scattered pion. The incident pion energy was 200 MeV and the angle of the scattered pions was 117.5°. As before the error bars represent statistical errors only. This momentum distribution is based on three runs with different though overlapping settings for the magnetic field of SUSI. The differential cross section for the momentum distributions is a true triple differential cross section. Each event was weighted to allow for the variation of the spectrometer acceptance with momentum. The cross sections have been corrected for the attenuation due to nuclear reactions in the target and in the windows, etc., of the apparatus, for pion decay losses, for muons counted as pions, and for wire chamber inefficiencies. By examining the proton data[4] which have smaller statistical errors, it was possible to check that the spectrometer acceptance function was correct and to estimate the systematic errors to be about 15%.

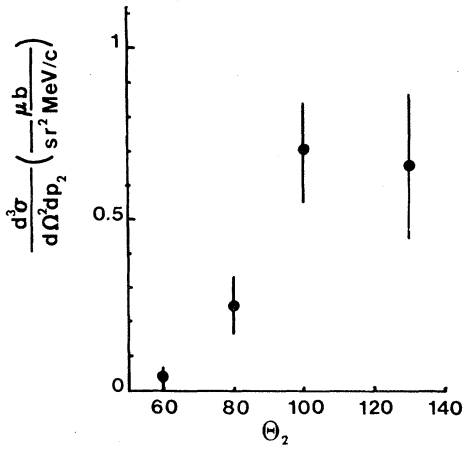

FIG. 7. Measured cross section versus θ_2 for the reaction ^{12}C$(\pi^+,\pi^+t)^9$B for $T_1 = 160$ MeV.

In Figs. 7–10, we present the measured angular and momentum distributions for the reactions ^{12}C$(\pi^\pm,\pi^\pm t)^9$B. These results complement the ones published earlier.[1] In view of the poor statistical definition of these data and the undoubtedly complicated nature of the $(\pi,\pi t)$ reaction we have not

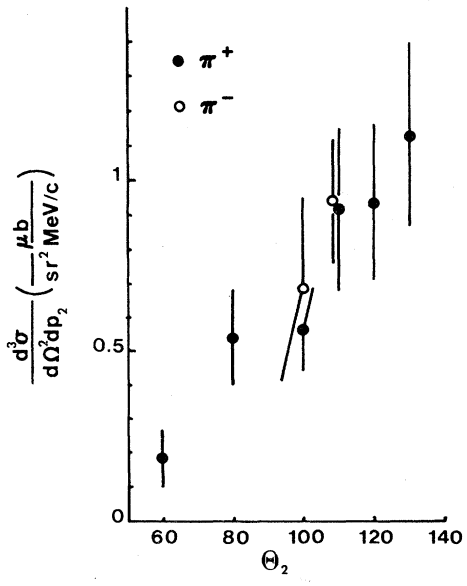

FIG. 8. Same as Fig. 7 except that $T_1 = 180$ MeV and π^- data are included.

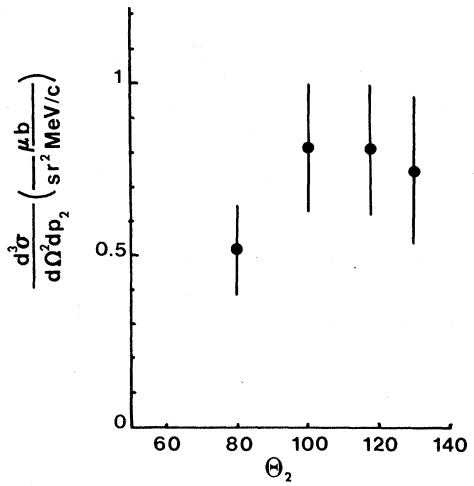

FIG. 9. Same as Fig. 7 but $T_1 = 200$ MeV.

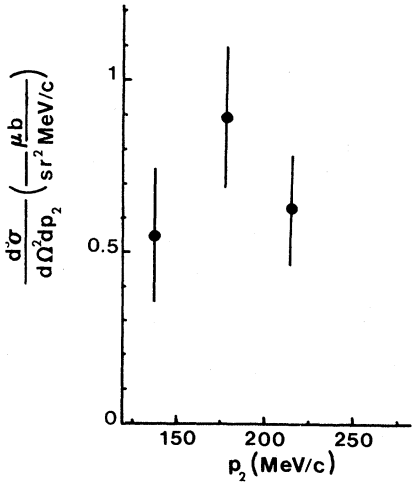

FIG. 10. Measured cross section versus p_2 for the reaction $^{12}C(\pi^+,\pi^+t)^{1}B$ for $T_1 = 200$ MeV and $\theta_2 = 117.5°$.

made any attempt to fit theoretical models to these distributions.

III. THEORETICAL MODELS

To describe the quasielastic $^{12}C(\pi^+,\pi^+d)^{10}B$ reaction with $E_{ex}(^{10}B) < 10$ MeV, we have considered two microscopic models: (1) the overlap shell model (one-step model); and (2) the internal pickup model (two-step model). These reactions are, respectively, represented by the reaction diagrams shown in Figs. 1(a) and 1(b). The dynamical contents of these two models are quite different. In the one-step model, one requires the formation of a virtual deuteron prior to the pion scattering. In the two-step model, the deuteron only forms in the final step of the reaction by an internal pickup process. As we shall see at the end of this section, this difference leads to different numerical results. The main purpose of our analysis is to see whether or not one needs to invoke preexisting deuteron clusters in ^{12}C in order to explain the observed high deuteron knockout rate. We have only performed plane-wave calculations of the diagrams of Fig. 1. As stated above, the effects of distortions amount more to a reduction of the absolute magnitude than to a change of the shapes of the differential cross sections.[6,7] We thus believe that our basis findings concerning the reaction mechanism will remain unchanged should distortions be included in future calculations.

The concept of the overlap shell model was first proposed in an early study of the $^{6}Li(p,pd)^{4}He$ reaction.[8] In this model, the projectile knocks out a preformed deuteron arising from the overlap of the single-particle wave functions of a neutron and a proton. In the present case, we describe the ^{12}C in terms of an ^{10}B core and a two-nucleon cluster composed of a proton and a neutron in the $1p_{3/2}$ shell. We then use the Brody-Moshinsky transformation[9] to transform the wave functions of these two particles into an internal wave function of the cluster and a wave function for the cluster relative to the ^{10}B core:

$$\langle l_1 l_2 m_1 m_2 \mid \lambda\mu\rangle \psi_{n_1 l_1 m_1}(\vec{x}_1)\psi_{n_2 l_2 m_2}(\vec{x}_2)\langle \tfrac{1}{2}\tfrac{1}{2} s_1 s_2 \mid SM_S\rangle = \sum_{nlNL}\sum_{mM}\langle lLmM \mid \lambda\mu\rangle\langle nl,NL,\lambda \mid n_1 l_1, n_2 l_2, \lambda\rangle \phi_{nlm}(\vec{r})\Phi_{NLM}(\vec{R})\langle \tfrac{1}{2}\tfrac{1}{2} s_1 s_2 \mid SM_s\rangle \,, \quad (1)$$

where $\langle nl,NL,\lambda \mid n_1 l_1, n_2 l_2 \lambda\rangle$ are the Brody-Moshinsky brackets.[9] All the other brackets are Clebsch-Gordan coefficients. The $(n_i l_i m_i s_i)$, $(i = 1,2)$, are the quantum numbers of the single particle state of the ith particle; the (nlm) and (NLM) are, respectively, the quantum numbers for the internal state of the cluster and the center of mass motion of the cluster in the parent nucleus; λ and S denote the total orbital momentum and the spin of the two particles[9];

$$\vec{r} \equiv (\vec{x}_1 - \vec{x}_2)/\sqrt{2}$$

and

$$\vec{R} = (\vec{x}_1 + \vec{x}_2)/\sqrt{2}$$

are, respectively, the internal coordinate of the clus-

ter and the coordinate of the center-of-mass of the cluster relative to the ^{10}B core. With $n_1=n_2=0$, $l_1=l_2=1$, we have for the quantum numbers $(nlNL)$ the possibilities (0010), (0101), (1000), (0002), and (0200). The internal wave function of the cluster is made to overlap the deuteron wave function. We only consider the s state ($l=0$) of the deuteron. This limits the above possibilities to those with $L=0$ and 2 only. Since S (the deuteron spin) $=1$, we have for $\vec{J}=\vec{L}+\vec{S}$ the possible values $\vec{J}=1,2,3$. Since

$$\vec{J}+\vec{J}_{\text{core}}=\vec{J}_{^{12}\text{C}}=0\ ,$$

this leads to three possible values for the spin of ^{10}B; $J_{\text{core}}=J=1,2,3$. Since the isospin of the deuteron is zero, the initial isospin of the (np) pair must also be zero. Consequently, the spin part of the initial (np) pair must be symmetric, which rules out $J_{\text{core}}=J=2$. This model predicts thus that only the $J=1$ ($T=0$) and $J=3$ ($T=0$) states of ^{10}B will be seen in this reaction. Currently, the resolution of our experiment is not sufficient to test this interesting prediction. The cross section in the one-step model is given by

$$\frac{d^3\sigma}{d\Omega^2 dp}=\tau\frac{d\sigma}{d\Omega}(\pi d)e^{-b^2k^2/2}G(k)\,|\int e^{i\vec{Q}\cdot\vec{r}}\,|\,\phi_d(\vec{r})\,|^2 d\vec{r}\,|^{-2}\ , \tag{2}$$

where

$$G(k)=\sum_{\alpha\beta}\{\Gamma_0(bk)[i_0(Q')]^2+\tfrac{3}{2}G_1^{0,\alpha}[i_1(Q')]^2+\Gamma_1(bk)i_0(Q')i_1(Q')\}\ , \tag{3}$$

with

$$\Gamma_0(x)=G_1^{0,\alpha}[\tfrac{3}{2}-x^2+x^4/6]+[G_1{}^{2,\alpha}+G_3{}^{2,\beta}]x^4/15$$

and

$$\Gamma_1(x)=C_1^{0,\alpha}[3-x^2]\ .$$

The constant terms predominate and the shape is similar to an S state wave function for the motion of the deuteron cluster. Further, we define

$$G_J^{L,\alpha}\equiv 28/(2J+1)(C_J^{L,\alpha})^2\ ,$$

where $C_J^{L,\alpha}$ is the coefficient of fractional parentage (cfp) for the αth state having total (orbital) angular momentum $J(L)$.[10] The numerical factor multiplying the cfp has its origin in the antisymmetrization (which was left out in the original formulation of the overlap shell model.[8]) The i_l are radial integrals over

$$W_l r^2 j_0(Q'r)\phi_d(r)f(r)\exp[-(r/2a)^2]\ ,$$

with $W_0=1$, $W_1=1-(r/2a)^2$, and j_0 is a spherical Bessel function. Here $\vec{Q}$ ($\vec{Q}'$) denotes half the pion momentum transfer in the πd (π^{12}C) c.m. system. The sums over α and β correspond to the first three excited states for each J, and the parameter b is related to the shell-model oscillator parameter by $b=a[A/(A-2)]^{1/2}$. For our case $A=12$ one obtains $a=1.69$ fm from electron scattering measurements. The term τ denotes the Jacobian of the transformation from the π^{12}C c.m. to the laboratory frame. The deuteron wave function ϕ_d and the correlation function f (which prevents the overlap of the nucleon cores within the cluster) are taken from Ref. 8. (The correlation parameter γ of Ref. 8 was varied over the given range $\gamma=0.75-2.0$. Our choice $\gamma=2.0$ was made because it gave the best agreement with our experimental results.) Finally we use for $(d\sigma/d\Omega)$ (πd) the experimental πd elastic cross sections of Ref. 11.

In the *two-step model* the pion is assumed to strike first a proton or neutron which then picks up another neutron or proton as it leaves the nucleus [See Fig. 1(b)]. This leads to the following differential cross section for the removal of an (np) pair from the p shell of ^{12}C:

$$\frac{d^3\sigma}{d\Omega_6 d\Omega_2 dP_2}=\tau'\sum_{\alpha,J_7,(T_7),m_7}\Big|\int d\vec{P}_3 X\sum_{\beta\delta\nu_5}G_{\alpha\beta\delta\nu_5,J_7(T_7)}\Phi_\beta f_{\nu_3,\nu_5}\theta(k_6-k_{58}-S_{np})\Big|^2\ , \tag{4}$$

where

$$X=\left[\frac{M_{23}}{2\pi^2 M_3}\right]\left[\frac{E_2''E_3''}{E_1''E_5''}\right]^{1/2}\left[\frac{E_8'}{4E_1'E_2'M_N}\right]^{1/2} \tag{5}$$

and

$$G_{\alpha\beta\delta\nu_5,J_7(T_7)}$$
$$\equiv[28/(2T_c+1)]^{1/2}C_{J_7(T_7)}\langle 1m_5\tfrac{1}{2}\nu_5 \mid \tfrac{3}{2}-\mu_4\rangle\langle \tfrac{3}{2}m_5\tfrac{3}{2}-m_5 \mid 00\rangle\langle 1m_8\tfrac{1}{2}\nu_8 \mid \tfrac{3}{2}\mu_8\rangle\langle \tfrac{3}{2}\mu_8 J_7\mu_7 \mid \tfrac{3}{2}\mu_4\rangle \ . \quad (6)$$

In Eqs. (4)–(6), the numerical subscripts refer to the particle numbers in Fig. 1(b). For example,

$$E_i\equiv(\vec{p}_i^{\,2}+M_i^2)^{1/2}$$

is the energy of the ith particle, M_N is the nucleon mass, and M_{23} is the invariant mass of the (23) pair. The single- and double-primed quantities denote, respectively, the energies calculated in the c.m. frames of the $\pi^{12}C$ and the π nucleon systems. Further, τ' is the Jacobian of the transformation of the the cross sections to the laboratory frame. The k_{58} and k_6 represent the kinetic energies of the (np) pair and the deuteron relative to the ^{10}B nucleus. Further,

$$S_{np}=M_p+M_n+M_{^{10}B}-M_{^{12}C}\simeq 27 \text{ MeV}$$

is the separation energy for the (np) pair from ^{12}C. The step function θ reflects the value of the minimum energy for deuteron knockout. For the sake of simplicity, we use $\alpha\equiv\{\nu_3,\nu_8\}$, $\beta\equiv\{m_5,m_8\}$, and $\delta\equiv\{\mu_4,\mu_5,\mu_7,\mu_8\}$ to denote the z components of the spin (ν), the orbital momentum (m), and the total angular momentum (μ) of the particles. In obtaining Eq. (4), we have carried out the summation over isospin indices, and T_7 is the isospin of the ^{10}B, which depends on the value of J_7. In Eq. (6) the brackets are the Clebsch-Gordan coefficients and $C_{J_7(T_7)}$ the cfp for separating an (np) pair from the $1p$ shell of ^{12}C and leaving the ^{10}B in a state with spin (isospin) of $J_7(T_7)$. Again

$$[28/(2T_c+1)]^{1/2}$$

is due to the antisymmetrization. The possible values for $J_7(T_7)$ are 3(0), 2(1), 1(0), and 0(1). Unlike the one-step model, it is now possible to have even-spin states for ^{10}B because the deuteron is now formed by an internal pickup process. Finally, in Eq. (4),

$$\Phi_\beta\equiv\psi_{3/2,m_5}(\vec{Q})\psi_{3/2,m_8}(\vec{Q}_1)\phi_d^*(\vec{Q}_2) \ ,$$

which is a product of two single-particle nucleon wave functions and the internal wave function of the deuteron, with

$$\vec{Q}=-\vec{P}_4-\vec{P}_1(A-1)/A \ ,$$

$$\vec{Q}_1-\vec{P}'_7+\vec{P}'_4(A-2)/(A-1) \ ,$$

and

$$\vec{Q}_2=\vec{P}_6/2-\vec{P}_3 \ .$$

The single-particle proton and neutron wave functions are the Fourier transforms of the p-shell wave functions used in the one-step model. The momentum space deuteron wave function is from Ref. 12.

IV. DISCUSSION

Results obtained with the use of the one- and two-step models are represented in Figs. 3–6 as solid and dashed curves, respectively. For ease of comparison with the experimental results, they have been multiplied by the numerical factors indicated in the figures. These curves should only be compared with the set of quasielastic data (shown as the crosses). As one can see both models are quite successful in reproducing the qualitative features of the various distributions.

In the two-step model, we have not included contributions to the cross section arising from a double-scattering term in which the pion scatters off both the proton and the neutron. This term is likely to be small because it represents a higher-order process. Its effects on calculated cross sections should be examined in the future when more detailed experimental information has become available. As explained at the beginning of Sec. III we believe that the qualitative features of our theoretical results discussed in this section will not be altered by the use of distorted waves in future calculations.

In its application to (p,pd) reactions, the overlap shell model gave an insufficient magnitude for the cross sections.[8] We believe this was due to the omission of a proper antisymmetrization of the many nucleon system in the original formulation of the model. In general, the antisymmetrization introduces an overall factor which is often quite important in reactions involving transfers of more than one nucleon.

The shapes of the angular distributions of the scattered pion given by the two models are quite different at large angles; they reflect essentially the difference between the differential cross sections of the πd and πp elastic scattering at these angles. The two models also give different positions of the maximum in the pion momentum distribution. However, current limited data points are not able to discriminate one against the other. Future experiments designed to distinguish these two models are called for.

ACKNOWLEDGMENTS

We appreciate the hospitality shown us by Prof. J. P. Blaser and his staff at the Schweizerisches Institut für Nuklearforschung. One of us, K.O.H.Z., wishes to thank the Alexander von Humboldt-Stiftung whose Senior American Scientist Award made this collaboration possible. This work was supported in part by the U. S. Department of Energy.

---

*Present address: EP Division, CERN, CH-1211 Geneva 23, Switzerland.

†Present address: Los Alamos National Laboratory, Los Alamos, NM 87545.

‡Present address: Physics Department, University of Texas, Austin, TX 78712.

§Present address: Laboratoire National Saturne, CENS, F-91191 Gif-sur-Yvette, France.

||Present address: Physics Department, University of Colorado, Boulder, CO 80302.

[1]R. J. Ellis, H. J. Ziock, K. O. H. Ziock, J. Bolger, E. Boschitz, J. Arvieux, R. Corfu, and J. Piffaretti, Phys. Lett. 88B, 253 (1979).

[2]R. Balsiger, B. Berkes, D. Brombach, D. George, M. Ianovici, E. Pedroni, I. Szavitz, M. Werner, J. Zichi, E. Boschitz, J. P. Egger, and C. A. Wiedner, Nucl. Instrum. Methods 157, 247 (1978).

[3]J. P. Albanese, J. Arvieux, E. T. Boschitz, R. Corfu, J. P. Egger, P. Gretillat, C. H. Q. Ingram, E. Lunke, E. Pedroni, C. Perrin, J. Piffaretti, L. Pflug, E. Schwartz, C. Wiedner, and J. Zichi, Nucl. Instrum. Methods 158, 363 (1979).

[4]H. J. Ziock, Ph.D. dissertation, University of Virginia, 1980.

[5]H. J. Ziock, R. J. Ellis, K. O. H. Ziock, J. Bolger, E. Boschitz, J. Arvieux, R. Corfu, and J. Piffaretti, Phys. Rev. C 24, 2674 (1981).

[6]L. C. Liu, Nucl. Phys. A223, 523 (1974).

[7]L. C. Liu, Helv. Phys. Acta 46, 201 (1973).

[8]Y. Sakamoto, Phys. Rev. 134, B1211 (1964).

[9]T. Brody and M. Moshinsky, *Tables of Transformation Brackets for Nuclear and Shell Model Calculations* (Gordon and Breach, New York, 1967).

[10]S. Cohen and D. Kurath, Nucl. Phys. A141, 145 (1970).

[11]K. Gabathuler *et al.*, Schweizerisches Institut für Nuklearforschung Report PR-80-011, 1980 (unpublished).

[12]W. Buck and F. Gross, Phys. Lett. 63B, 286 (1976).